Supplementary material

S1 Method material

S1.1 SFINCS Basemap

Figure S1 shows the SFINCS model domain with its elevation, in- and -outflow boundaries and output points for timeseries analyses. SFINCS uses the simulated wflow discharge as input for the fluvial flooding, and the D-Flow FM – SnapWave simulated coastal water levels as input for the coastal flooding.

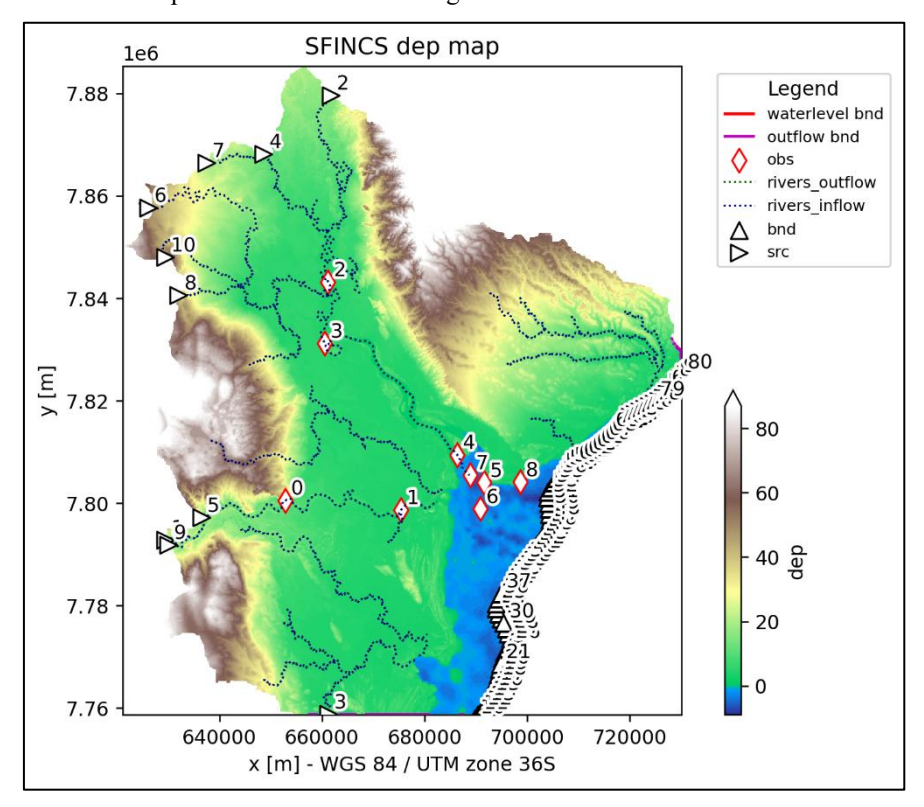


Figure S1: Basemap of the local SFINCS model with the boundary conditions coupling the wflow discharge output (src), water level boundary coupling the D-Flow FM – SnapWave output (bnd), outflow boundary (outflow bnd), rivers, elevation (dep), and the SFINCS output points for timeseries data (obs).

S1.2 Wflow bankfull discharge

Figure S2 shows the estimated return values for extreme discharge in the two largest rivers, the Buzi (Gauge 1) and the Pungwe (Gauge 2), see Figure S1 for gauge locations. The 2-year return period is estimated for all gauges (Table S1) and removed from the wflow simulated discharge of the event (example for the Buzi river in Fig. S3). The 2-year return period represents

an approximation of the bankfull river discharge and this relationship is based on semi-empirical relationships (Liu et al., 2024). Due to the lack of river bathymetry data, we remove the bankfull discharge from the discharge boundary conditions for SFINCS and assume that the incoming discharge represents out of banks discharge, thereby removing the need to burn in an (unknown) river conveyance in the digital elevation model. This approach may lead to an under- or overestimation in river discharge input for our SFINCS model simulations.

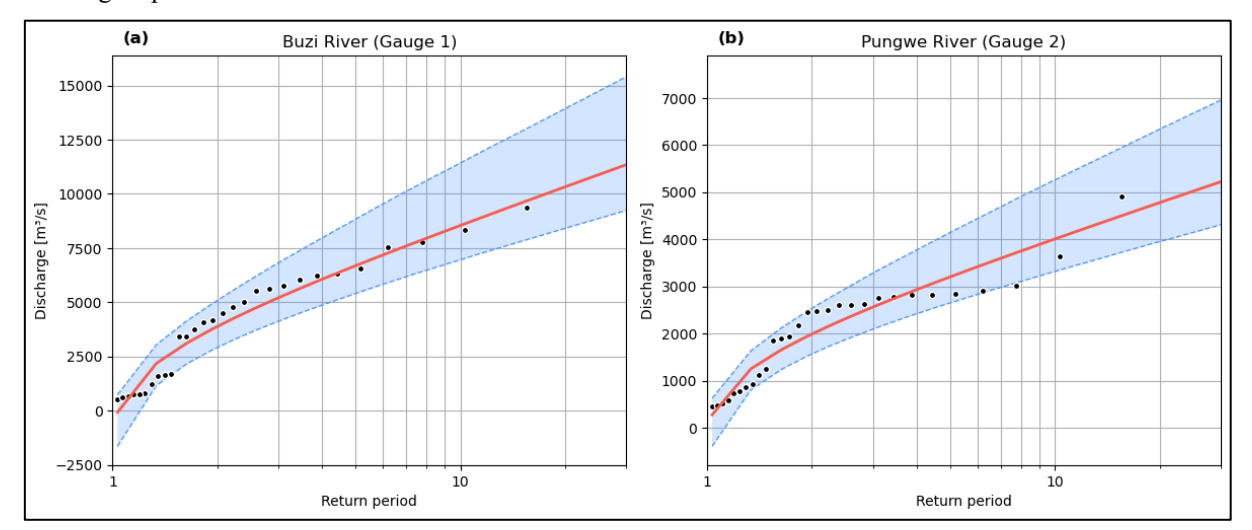


Figure S2: The estimated return values for maximum discharge (m³/s) in the Buzi (a) and the Pungwe (b) rivers, based on an extreme value analysis (Bocharov, 2023) using block maxima for a 30 year wflow simulation (1989-2019). The fit (red) and confidence interval (95%; blue) are plotted next to the annual maxima.

Table S1: The estimated 2-year return period (bankfull discharge) in m³/s from a 30 year wflow simulation (1989-2019) for all discharge boundary points of the SFINCS model domain (see Fig. S1 for locations), together with the upper and lower 95% confidence intervals (CI) in m³/s.

Gauge	Bankfull	Lower 95%	Upper 95% CI (m³/s)	
ID	Discharge (m³/s)	CI (m ³ /s)		
1	3887	2935	5140	
2	1992	1579	2532	
3	102	72	181	
4	179	135	235	
5	197	141	275	
6	99	70	157	
7	30	23	40	
8	15	11	28	

9	89	63	124
10	8	7	13

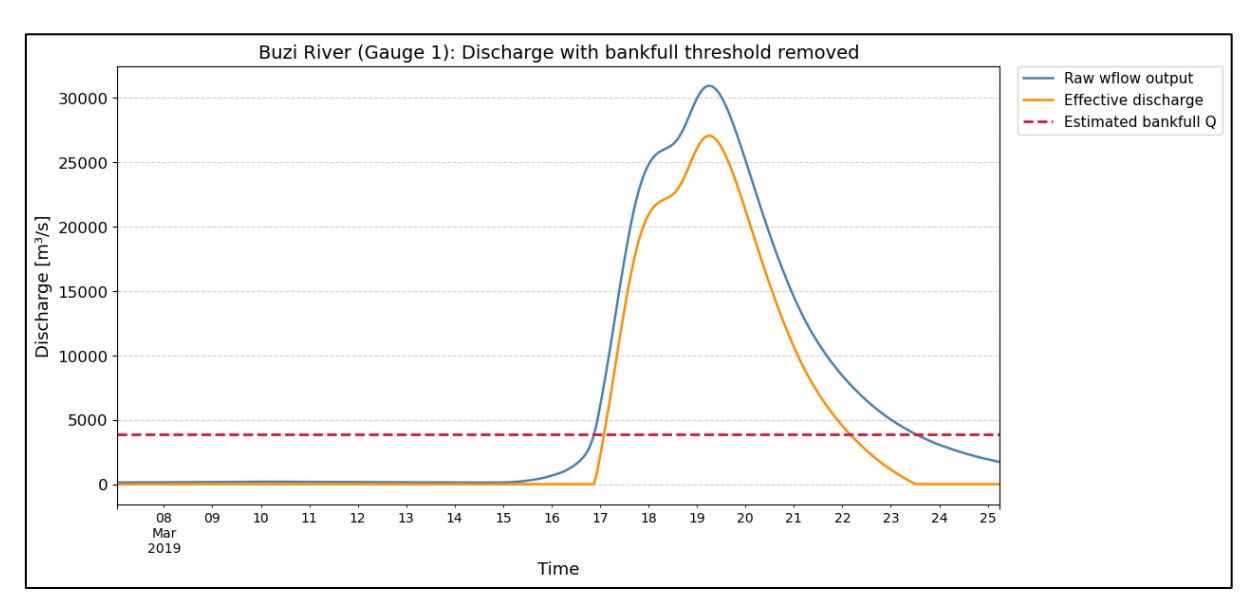


Figure S3: Example of bankfull discharge removal for the Buzi river (Gauge 1) for the period of TC Idai. The estimated 2-year return period (red) is removed from the wflow output (blue) to correct for missing river bathymetry before provided as discharge boundary to SFINCS.

S1.3 Simulated discharge comparison with GRDC stations

The same wflow model as for Sect. 1.2 is run for 30 years that align with the available Global Runoff Data Centre (GRDC) discharge data (The Global Runoff Data Centre, 2025) within the region (1954-1984, Fig. S4), using ERA5 daily rainfall and temperature forcing. The climatology and 30-year daily timeseries for GRDC stations closest to the SFINCS model domain are compared to the wflow data (Figs. S5 and S6). The seasonality and long term dynamics are simulated reasonable to well (KGE 0.28 and 0.87 for the Pungwe and Buzi rivers, respectively) but the extremes are generally overpredicted.

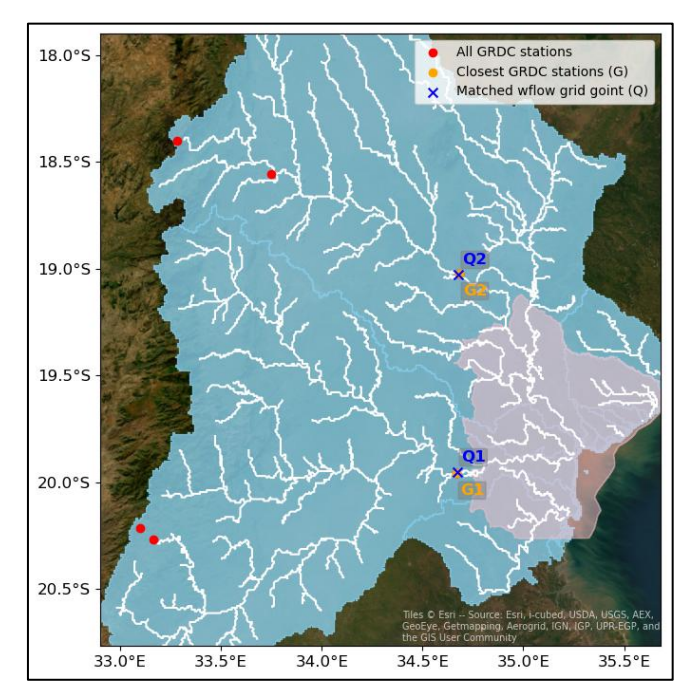
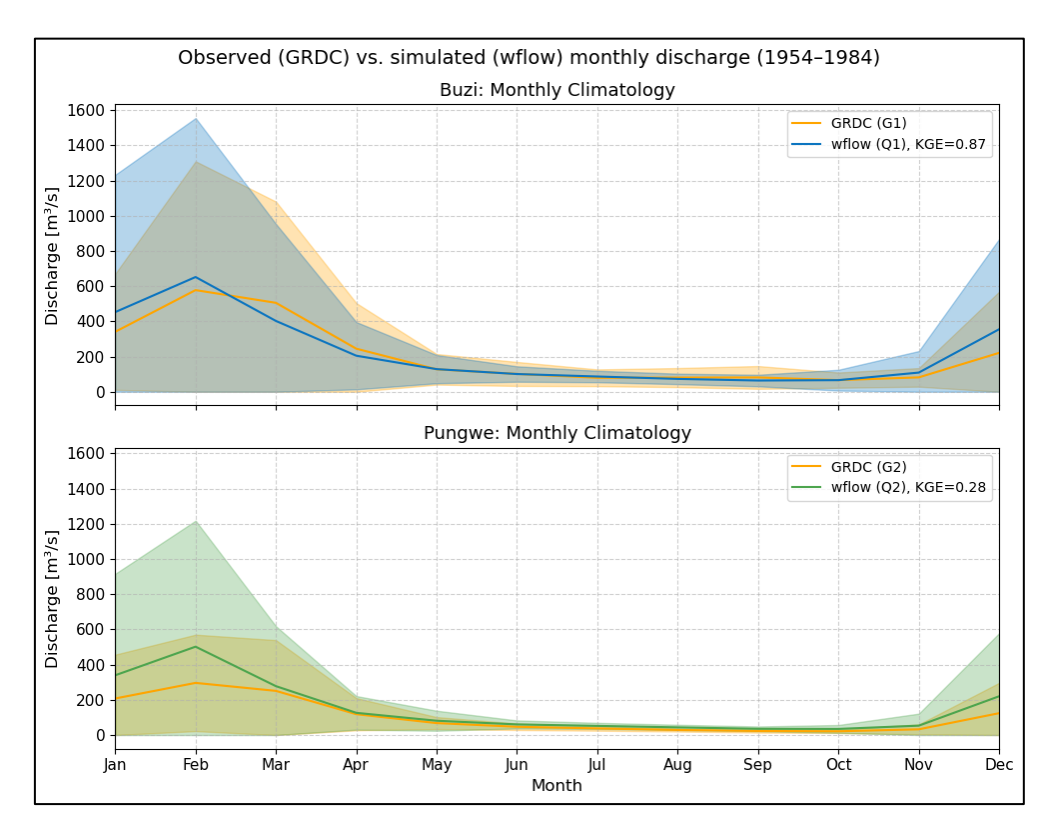


Figure S4: The selected GRDC gauges (blue) and closest wflow grid points (orange) to compare historical discharge in the Sofala province, Mozambique, for the Buzi (G1 and Q1), and Pungwe (G2 and Q2) rivers. The wflow and SFINCS domains are shown in blue and pink, respectively, as well as the river geometries in white.



45 Figure S5: The monthly mean discharge (climatology) in m³/s for the Buzi (a) and the Pungwe (b) rivers, using the GRDC discharge data and a 30-year wflow simulation for the GRDC available stations within the Sofala region and available time period (1954-1984).

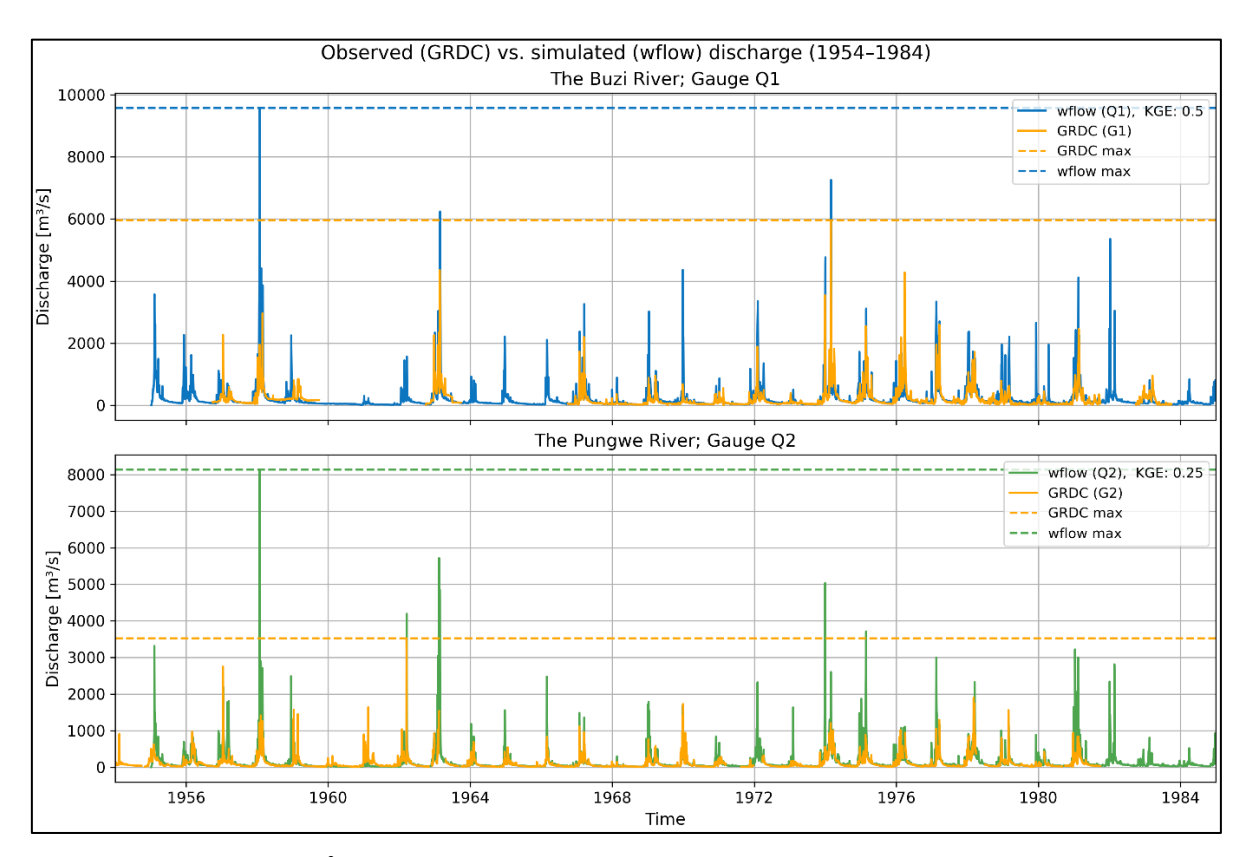


Figure S6: The daily discharge in m³/s for the Buzi (a) and the Pungwe (b) rivers, using the GRDC discharge data (1954-1984) and corresponding wflow simulation performed at the daily timestep, available stations within the Sofala region and available time period (1954-1984).

S1.4 SnapWave

50

55

Figure S7 shows which SnapWave coastal transects are matched to D-Flow FM output points. Ideally, SnapWave would be fully integrated into the SFINCS model to prevent potential wave dissipation due to the shallow and sloping coast; however, this was not yet possible at the time of preparation of this paper. For station 62 (panel b), as for many other stations, the maximum wave setup does not totally align in time with the maximum water level from tide and surge due a time mismatch (up to 30 min) resulting from the spatial difference between the D-Flow FM and SnapWave output.

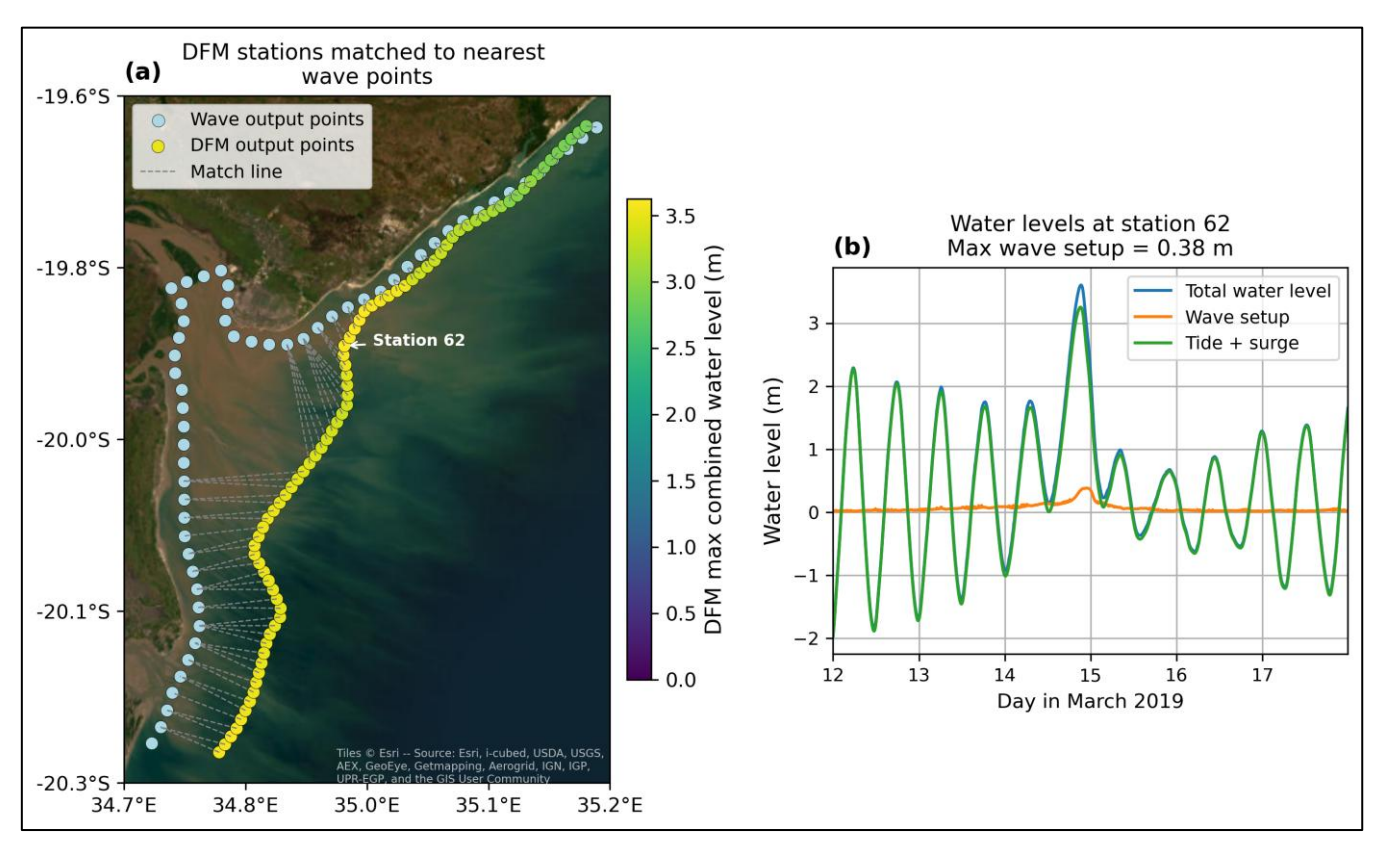


Figure S7: Panel a shows the output points of SnapWave (blue) matched to the D-Flow FM output points, depicted with their total water level value (viridis scale), to add the simulated wave setup to the simulated tide and surge. Panel b shows an example of the simulated total water level (blue) after adding wave setup (orange) to tide and surge (green) for the period of 12 to 17 March 2019 at station 62, which is the station closest to Beira.

S1.5 Flood map satellite comparison

65

The simulated factual flooding from our SFINCS model simulations is compared to the satellite-derived flood extent for TC Idai from UNOSAT (https://unosat.org/products) and CEMS (https://portal.gfm.eodc.eu/; Fig. S8). Several metrics are used to compare our simulated flooding with that derived from the satellite products, based on Eilander et al. (2023). The critical success index (C) is the ratio between the correctly classified instances and the union of both error and correct instances. The hit rate (H) is the proportion of observed flooding that is correctly estimated by the model. The false-alarm ratio (F) is the proportion of modelled flooded area that is not flooded in the observation dataset.

We find a good hit rate when comparing the estimated flooding to both satellite products (> 76%), but a poor false-alarm ratio for the CEMS comparison (60 %). The critical success index is better for the UNOSAT (68 %) than for the CEMS (40 %) comparison. Important to note is the large difference in detected flood extent between the two satellite products, highlighting the lack of "truth". For the region North East of Beira, we underpredict flooding compared to the UNOSAT product but

overestimate compared to the CEMS product. This area might be difficult to observe due to the larger elevation gradient with forest transitioning to grass- and cropland (Lisboa et al., 2024).

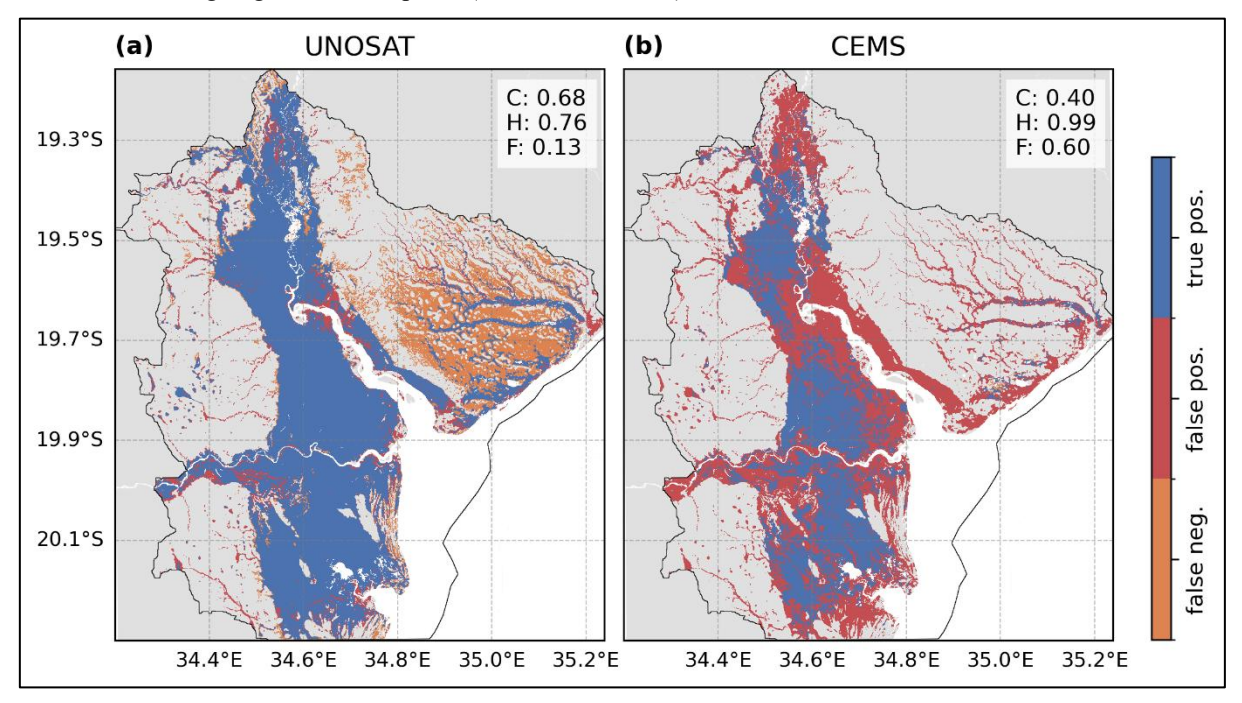


Figure S8: Our factual maximum flood depth simulations compared to satellite observed flood extent of UNOSAT (a) and CEMS (b). The agreement between the model and satellite products is expressed using the critical success index (C), hit rate (H) and false-alarm ratio (F), based on Eilander et al. (2023).

S1.6 Counterfactual forcing

80

85

For the counterfactual rainfall scenario, every rainfall value is multiplied by 0.92 to remove the plausible 8% of increased rainfall due to climate change from the factual data.

For the counterfactual wind scenario, the maximum sustained wind speed (U_{max}) along the track is adjusted using the counterfactual wind value (CF_{wind}) of 10 %, following the methodology of Mester et al. (2023):

$$U_{\text{max }_CF} = U_{max} * 1 + \frac{1}{cF_{wind}}, \tag{S1}$$

Also the pressure is adjusted accordingly, where the minimum pressure (P_{min}) along the track is increased with the product of the inverse of the counterfactual wind value (CF_{wind}) and the pressure difference between P_{min} and the environmental pressure $(P_{env}, \text{Eq. S2})$. The new wind and pressure values are used to create counterfactual wind and pressure fields for Idai.

90
$$P_{min_CF} = P_{min} + -1 * \frac{1}{CF_{wind}} * (P_{env} - P_{min})$$
 (S2)

For the counterfactual SLR scenario, the SLR is removed from the tidal boundary conditions and initial water level of D-Flow FM using the Python package dfm_tools for pre- and postprocessing of model in- and output files (Veenstra, 2025). Five stations are selected along the coast of Mozambique, within the D-Flow FM domain. The SLR of these stations is averaged. As mentioned in Section 2.1.3, GEBCO v2024 is used to determine the ocean's bathymetry and thereby implicitly the sea level. The ocean depth is referenced to m.s.l., yet the temporal dimension (i.e. reference year) of this mean sea level is not defined. As the development of global bathymetry datasets started in the mid-1990 thanks to the advancement of satellite altimetry (Tozer et al., 2019), we assume that the m.s.l. measured then is the vertical datum still used today. Therefore, we analyse the mean regional SLR from the ISIMIP Hourly Coastal water levels with Counterfactual (HCC) dataset (Treu et al., 2024) for 1990 – 2000 and add the difference between then and 2019 (4 cm) to the tidal boundary and initial water level of the factual scenario. The difference between 1901 (start of the dataset) and the 1990 – 2000 mean (10 cm) is subtracted from the tidal boundary and initial water level for the counterfactual scenario, leading to a 14 cm difference between the factual and counterfactual scenario. Global bathymetry data inaccuracies can vastly surpass the size of SLR (Tozer et al., 2019) and advancements of local bathymetry data are crucial to accurately estimate the effect of SLR.

100

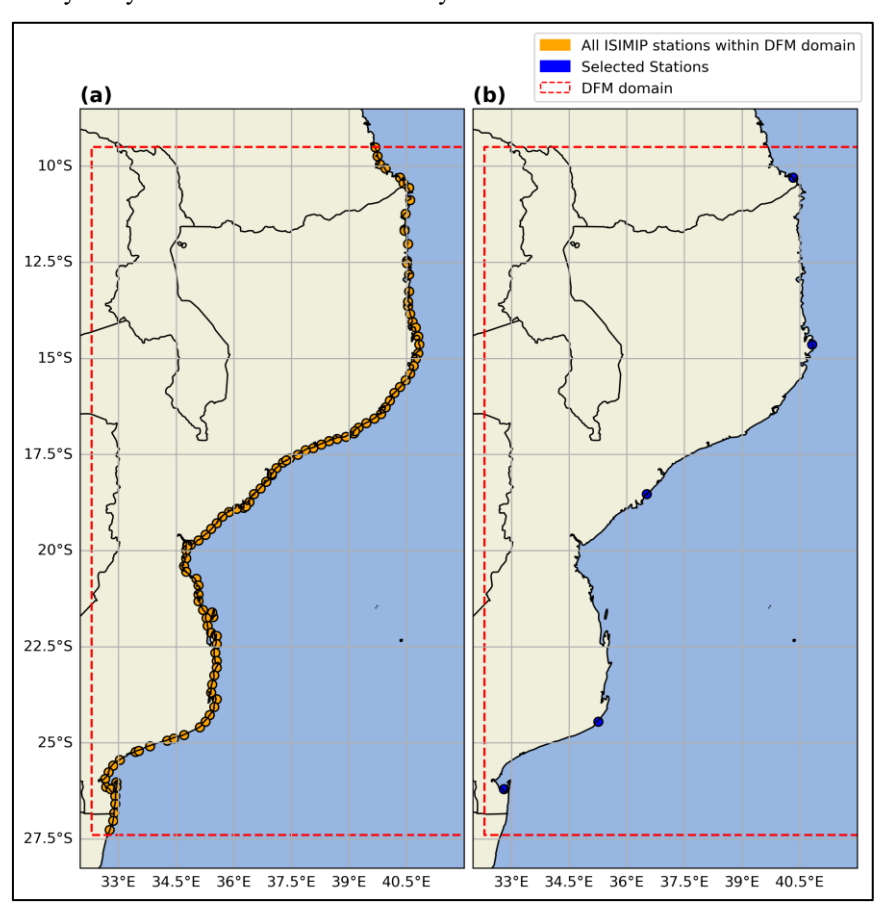


Figure S9: All stations of the ISIMIP HCC dataset within the D-Flow FM (DFM) model domain (left) and the selected five stations used to average the regional SLR (right).

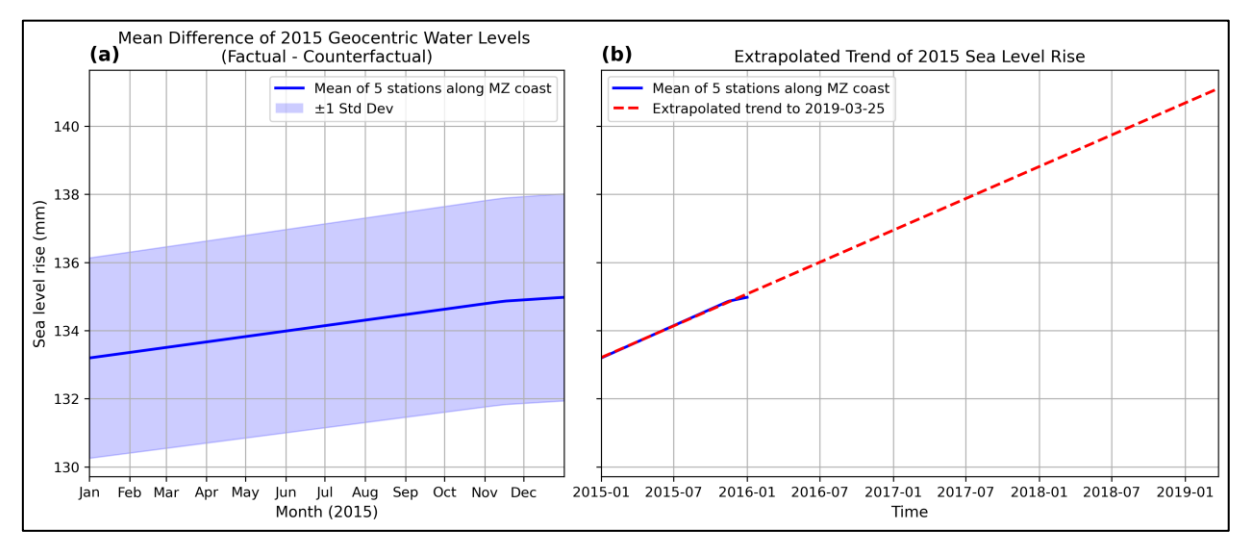


Figure S10: Since the ISIMIP HCC dataset ends in 2015, we assume a linear trend and extrapolate the regional SLR average of the five stations along the coast of Mozambique (Fig. S9) to March 2019, when TC Idai took place.

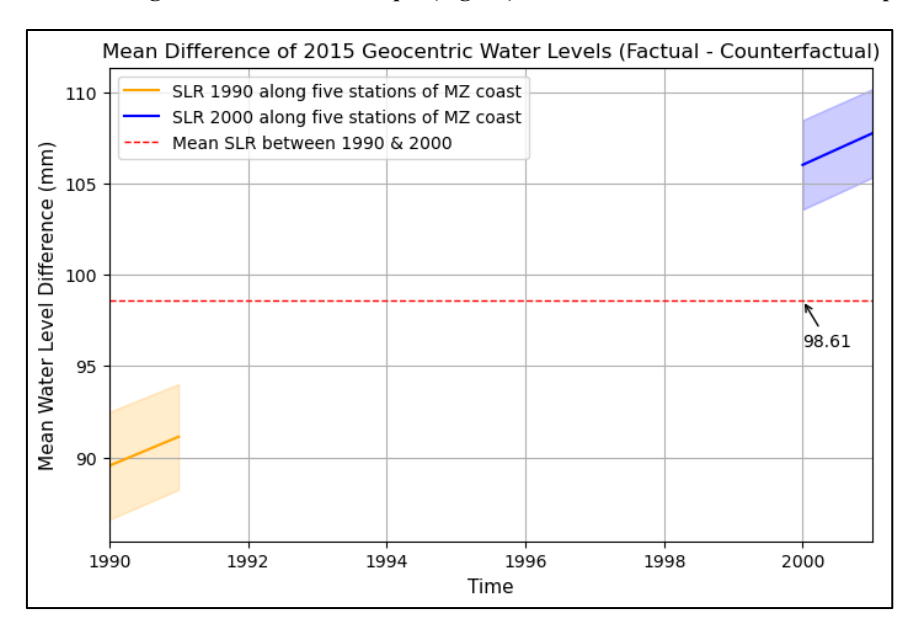


Figure S11: To calculate the implicit SLR in the GEBCO bathymetry dataset, we calculate the mean of the SLR averaged of the five stations along the coast of Mozambique (Fig. S9) for 1990 and 2000 from the ISIMIP HCC dataset.

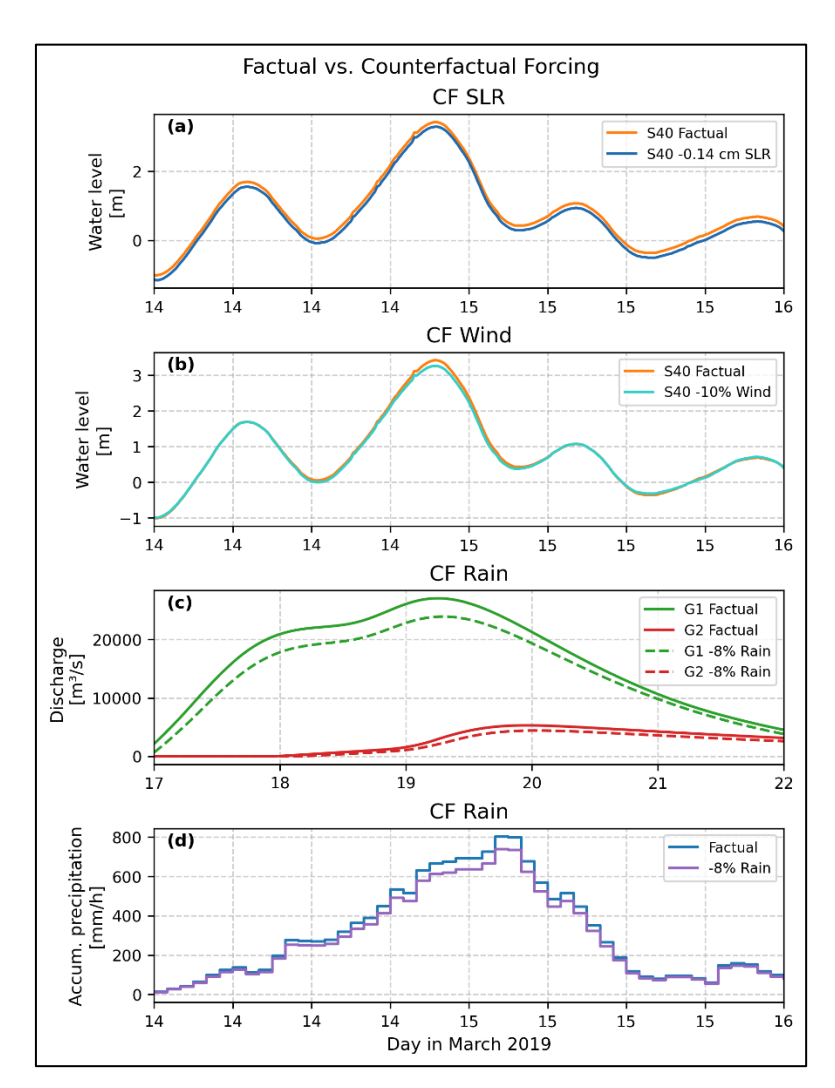


Figure S12: The factual and counterfactual (CF) time series data for the change in SLR and wind at a coastal water level boundary point (S40, see Fig S13 for location; panels a and b), the change in rain for two discharge boundary points of the Buzi (G1) and Pungwe (G2) rivers (panel c; for locations see Fig S13), and for change in accumulated rainfall over the SFINCS model domain (panel d). Panel c has a different x axis to better capture the timing range of the factual and counterfactual peak discharge.

S2 Supplementary result figures

120

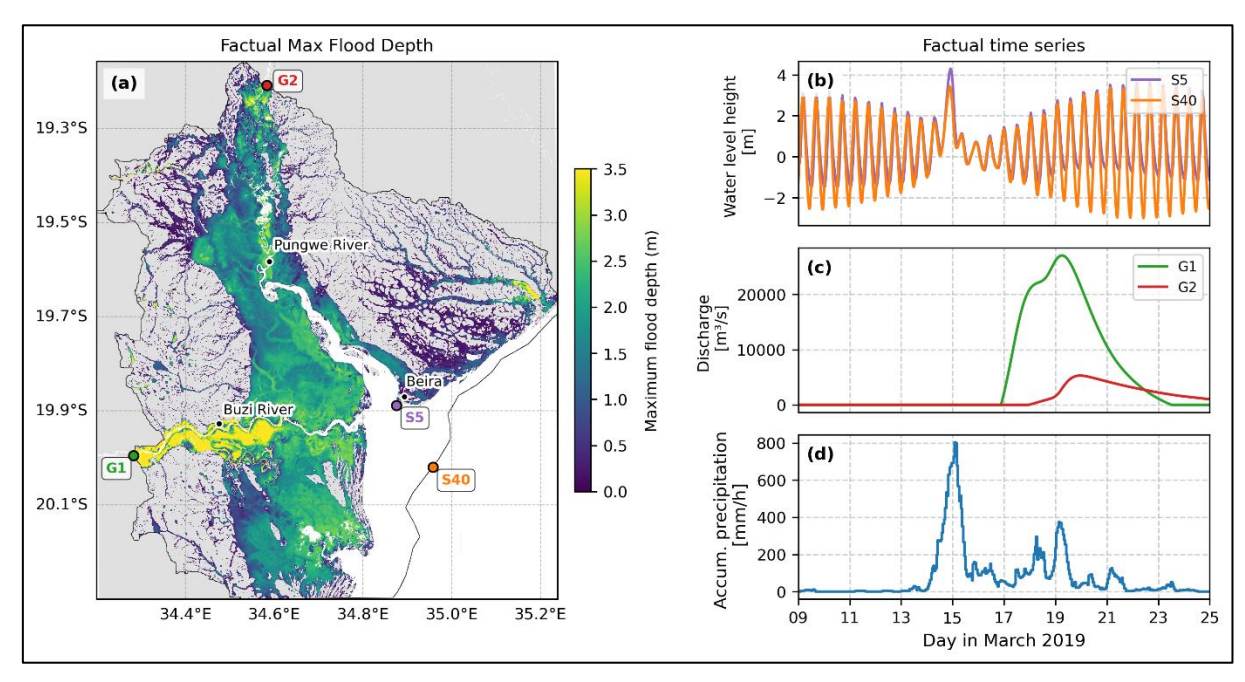
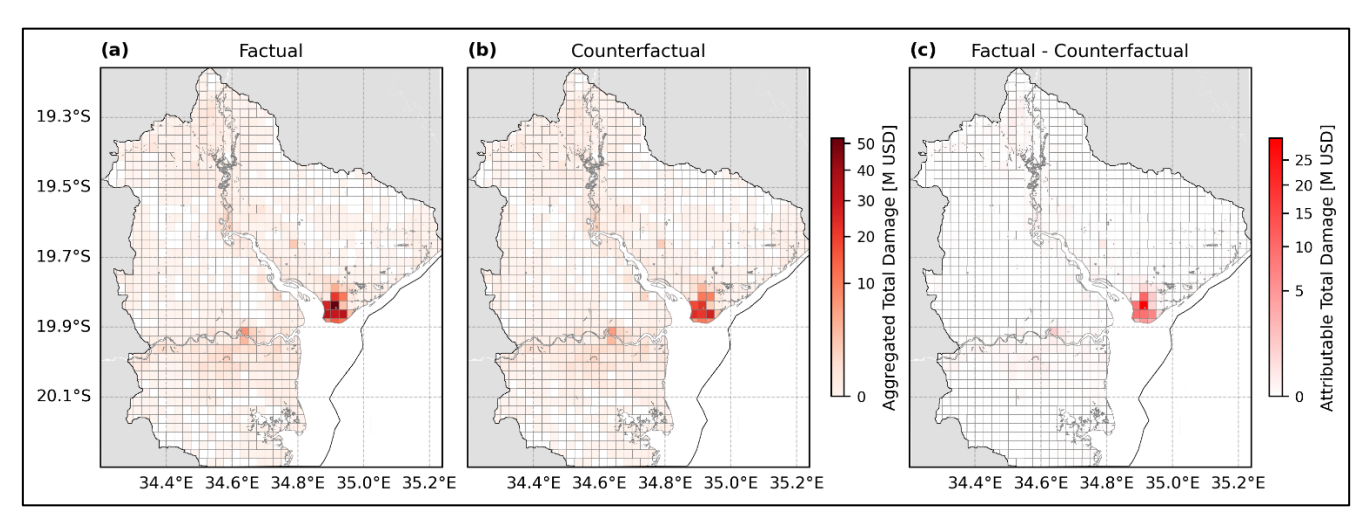


Figure S13: The factual simulated maximum flood depth in meters from TC Idai (a), and the factual forcing over time for coastal water levels at two stations (S5 and S40; b), discharge in m³/s at the Buzi (G1) and Pungwe (G2) rivers (c), and accumulated rainfall over the SFINCS model domain in mm/hour from ERA5 (d). The SFINCS model domain is shown in black in panel (a).

Table S2: The absolute and relative change in flood volume, flood extent and flood damage for factual (absolute values only) and counterfactual scenarios for all driver combination, including more than in Table 2. The relative change in flooding and impact that is attributable to climate change is calculated by applying Eq. 1.

Scenario	Flood volume		Flood ext	Flood extent		Flood damage	
	Absolute value	Relative	Absolute value	Relative	Absolute value	Relative	
	$[M m^3]$	change	[km²]	change	[M USD]	change	
Factual	5502	-	3592	-	349	-	
Counterfactual							
Rain	5023	8,69 %	3526	1,83 %	334	4,17 %	
SLR	5488	0,24 %	3590	0,08 %	313	10,22 %	
Wind	5474	0,51 %	3577	0,43 %	280	19,65 %	
Rain & SLR	5010	8,94 %	3523	1,92 %	297	14,68 %	
Rain & Wind	4996	9,20 %	3510	2,28 %	264	24,23 %	
SLR & Wind	5463	0,70 %	3574	0,51 %	256	26,60 %	
All	4984	9,40 %	3507	2,36 %	240	31,16 %	



130 Figure S14: The aggregated (0.025° grid cells) total damage for the factual (a) and counterfactual (b) scenarios with all drivers combined, and the absolute difference attributable to climate change (c). The compound flood model (SFINCS) domain is shown in black.

References

- 135 The Global Runoff Data Centre: https://portal.grdc.bafg.de/, last access: 2 July 2025.
 - Bocharov, G.: pyextremes (Version 2.3.3), https://github.com/georgebv/pyextremes, 2023.
 - Eilander, D., Couasnon, A., Leijnse, T., Ikeuchi, H., Yamazaki, D., Muis, S., Dullaart, J., Haag, A., Winsemius, H. C., and Ward, P. J.: A globally applicable framework for compound flood hazard modeling, Natural Hazards and Earth System Sciences, 23, 823–846, https://doi.org/10.5194/nhess-23-823-2023, 2023.
- Lisboa, S. N., Grinand, C., Betbeder, J., Montfort, F., and Blanc, L.: Disentangling the drivers of deforestation and forest degradation in the Miombo landscape: A case study from Mozambique, International Journal of Applied Earth Observation and Geoinformation, 130, 103904, https://doi.org/10.1016/j.jag.2024.103904, 2024.
 - Liu, Y., Wortmann, M., Hawker, L., Neal, J., Yin, J., Santos, M. S., Anderson, B., Boothroyd, R., Nicholas, A., Smith, G. S., Ashworth, P., Cloke, H., Gebrechorkos, S., Leyland, J., Zhang, B., Vahidi, E., Griffith, H., Delorme, P., McLelland, S.,
- Parsons, D., Darby, S., and Slater, L.: Global Estimation of River Bankfull Discharge Reveals Distinct Flood Recurrences Across Different Climate Zones, https://doi.org/10.21203/RS.3.RS-5185659/V1, 2024.
 - Mester, B., Vogt, T., Bryant, S., Otto, C., Frieler, K., and Schewe, J.: Human displacements from Tropical Cyclone Idai attributable to climate change, Hazards Earth Syst. Sci, 23, 3467–3485, https://doi.org/10.5194/nhess-23-3467-2023, 2023.

- Tozer, B., Sandwell, D. T., Smith, W. H. F., Olson, C., Beale, J. R., and Wessel, P.: Global Bathymetry and Topography at 15 Arc Sec: SRTM15+, Earth and Space Science, 6, 1847–1864, https://doi.org/10.1029/2019EA000658, 2019.
 - Treu, S., Muis, S., Dangendorf, S., Wahl, T., Oelsmann, J., Heinicke, S., Frieler, K., and Mengel, M.: Reconstruction of hourly coastal water levels and counterfactuals without sea level rise for impact attribution, Earth Syst Sci Data, 16, 1121–1136, https://doi.org/10.5194/ESSD-16-1121-2024, 2024.
- Veenstra, J.: dfm_tools: A Python package for pre- and postprocessing D-FlowFM model input and output files (v0.35.0),
- 25. Zenodo, https://doi.org/10.5281/zenodo.14901200, 2025.